



## Enhancing Performance of an Air Conditioner by Preheating and Precooling of Liquid Desiccant and Non-processed Air

B. Ebrahimpour<sup>a</sup>, A. Moazemi Goudarzi<sup>\*b</sup>, A. Kaviani<sup>c</sup>

<sup>a</sup> Faculty of Technology, University of Portsmouth, Portsmouth, United Kingdom

<sup>b</sup> Department of Mechanical Engineering, Babol Noshirvani University of Technology, Babol, Iran

<sup>c</sup> Faculty of New Sciences and Technologies, University of Tehran, Tehran, Iran

### P A P E R I N F O

#### Paper history:

Received 10 May 2021

Received in revised form 27 November 2021

Accepted 04 December 2021

#### Keywords:

Moisture Content

Liquid Desiccant Air Conditioner

Lithium Chloride

Counter-flow Enthalpy Exchanger

Optimization

Particle Swarm Optimization

### A B S T R A C T

Corrosive fluids such as lithium chloride are often used in liquid desiccant air conditioners. Corrosion in enthalpy exchanger is one of the design problems. Some solutions are studied in this research, and based on them; an experimental setup is investigated. In this design, a counter-flow enthalpy exchanger is used to exchange moisture between the air and the liquid desiccant. First, the inlet air is preheated or pre-cooled by an aluminium heat exchanger. Then, the liquid desiccant is preheated or pre-cooled by thin-walled plastic tubes. By contacting this processed air and liquid desiccant, heat, and mass exchanging occurs. The variation of the air moisture content is investigated in laboratory conditions, and the rate of regeneration and dehumidification is studied. The results indicate that in general, the ambient air moisture content decreased around 20% during the dehumidification process and it enhanced around 14.28% during the regeneration process. Furthermore, the moisture content variation in the dehumidification process improved at least 9.92%, but the regeneration process decreased at least 10.76% compared to the previous study. In addition, utilizing the particle swarm optimization algorithm is desirable to identify the system's transient behavior and obtain the fitting parameters of a curve that is closely similar to the experimental data of the rate of dehumidification and regeneration and the average errors of the fitted curve were 10.43 and 1.52%, respectively.

doi: 10.5829/ije.2022.35.02b.19

## 1. INTRODUCTION

Although air conditioners were considered luxury products in the past, these days, they have become a necessity of human life [1]. Rising living standards, advances in technologies, and population growth have caused about 15% of the world's energy to be used by air conditioners [2]. The air conditioners in use are almost the vapor compression type, which has low efficiencies and use of CFC, HCFC, and HFC refrigerants. These refrigerants are used to cool water in evaporators, and over time, due to their leakage into the atmosphere, they react with ozone in the stratosphere. They also need fossil fuels and a large amount of electricity. Therefore, due to

the energy crisis and the destruction of nature, researchers have turned to other methods, including desiccant cooling systems (DCS). The optimal desiccant should have a high moisture absorbing capacity and, at the same time, a lower regeneration temperature [3]. Desiccant cooling systems include solid or liquid desiccant. Solid desiccants are inexpensive, non-flammable, non-corrosive, and environmentally friendly and regenerate faster than liquid desiccants. However, they consume more energy. Unlike liquid desiccants, dehumidification and regeneration in solid desiccants are usually done simultaneously [4].

Liquid Desiccant systems (LDSs) usually consist of components such as dehumidifier, liquid desiccant,

\*Corresponding Author Institutional Email: [goudarzi@nit.ac.ir](mailto:goudarzi@nit.ac.ir)  
(A. Moazemi Goudarzi)

regenerator, and packing material. Liquid desiccants such as lithium chloride, lithium bromide [5], and other salts are corrosive. Any transfer of liquid desiccant with the airflow (carryover) can seriously damage the habitant's health. Corrosion and carryover, which are the main problems of these systems, can be solved using plastic materials and microporous membranes as semi-permeable membranes, respectively.

Important properties of liquid desiccants include conductivity, dynamic viscosity, specific heat capacity, density, and surface vapor pressure. The materials with low vapor pressure are LiCl, LiBr, and CaCl<sub>2</sub>, in which LiCl has the minimum vapor pressure.

Nowadays, the general policies of countries are to reduce energy consumption and use of renewable resources. Renewable energies such as solar energy [6] and wind energy [7] can generate the energy demanded in LDAC systems. Alizadeh and Saman [8] studied a solar collector's thermal performance as a regenerator and used a computer model for CaCl<sub>2</sub>. They found that the theoretical model and experimental results had a good agreement [9]. Qiu et al. [10] used a system with a biomass boiler that supplied 554 Watts for regeneration. In this study, HCOOK was used which reduced the relative humidity by up to 13% for humid air. Turgut and Çoban [11] also conducted an experimental and numerical study and evaluated LiBr and LiCl dehumidification rates. The results indicated that LiCl had a higher dehumidification rate. In a theoretical and experimental research, Mohamed et al. [12] observed that the dehumidification was increased up to 1.33 times by increasing the packing length from 0.5 m to 1 m. Peng et al. [13] compared the efficiency of a system containing LiCl or CaCl<sub>2</sub>. LiCl has about 60% more efficiency and 16% lower exergy efficiency compared to CaCl<sub>2</sub>.

In the previous studies, various factors on a liquid desiccant air conditioner (LDAC) system were investigated. The fluid inlet temperature is an important parameter in a dehumidification process. Using a mathematical model for an LDAD system, Lu et al. [14] observed that as the inlet solution temperature increases, the ratio of outlet moisture and outlet air temperature increases. In a previous research, Moazemi et al. [15] were investigated an LDAC system with LiCl to reduce the effect of carryover.

This study proposes an innovative configuration of an LDAC system with LiCl in which preheating or precooling of the air and the liquid desiccant is done simultaneously. The effect of this new configuration on the variation of temperature, relative humidity, moisture content during the dehumidification and regeneration processes was studied and additionally, with the help of particle swarm optimization (PSO) algorithm, the system's transient behavior is determined.

## 2. SYSTEM DESCRIPTION

The corrosive of LiCl is one of the main limitations for the design of an LDAC system with LiCl desiccant. For instance, in an LDAC system with LiCl desiccant, a plate heat exchanger and pumps were made of stainless steel. After a few years, corrosion was visible in the system, which is shown in Figure 2. As a multi-criteria target, it is necessary to consider different strategies that find the best solution for this specific problem [16]. There are two different strategies that are adopted to deal with corrosion of the liquid desiccant. According to Figure 1, in the first strategy, to avoid corrosion, the liquid desiccant is not preheated or precooled, and only the inlet air passing through the enthalpy exchanger is preheated or precooled. In the second strategy, utilizing a polymer enthalpy exchanger, the liquid desiccant is also preheated or precooled, as well as the inlet air.

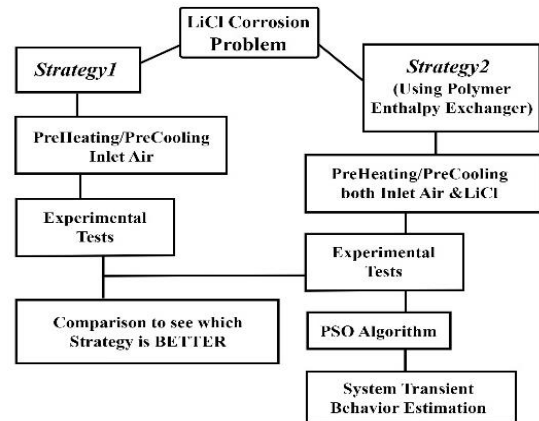


**Figure 1.** The flowchart of different strategies for LiCl corrosion problem in this research

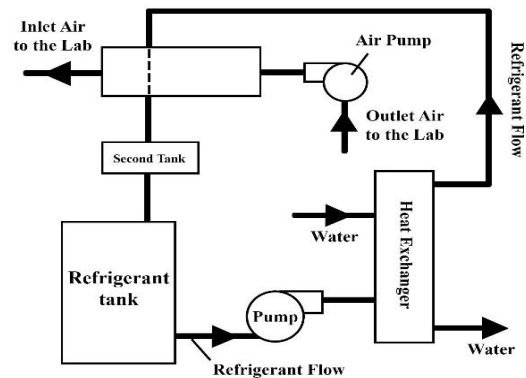


**Figure 2.** The schematic of liquid desiccant air conditioner with LiCl installed in Babol Noshirvani University of Technology

The first strategy was investigated in the previous study. Accordingly, the second strategy was chosen in this study and an LDAC system with LiCl was investigated, which is shown in Figure 3. A polymer counter-flow enthalpy exchanger was used for exchanging moisture content between the air and the liquid desiccant. Depending on the conditions, whether it is the dehumidification process or regeneration process, the inlet air passing through the enthalpy exchanger is pre-cooled or pre-heated by an aluminium heat exchanger in which water flows in it. Utilizing thin-walled plastic tubes in the liquid desiccant bed, LiCl can be pre-heated or pre-cooled simultaneously with the inlet air. Figure 3 depicts that the components of the experimental setup. The counter-flow enthalpy exchanger was made of 5 vertical-multi-channel polypropylene blocks for increasing the contact of desiccant and air. Each block had a dimension of  $50 \times 50 \times 10 \text{ cm}^3$  at intervals of 1 cm from each other, and their channels had a size of  $4 \times 4 \text{ mm}^2$  at a thickness of 0.5 mm.

According to Figure 4, the inlet air at point 1 exchanges heat with the aluminium heat exchanger, which there is a flow of water in its coil, then exits at point 2. The processed air enters the enthalpy exchanger tower from downwards and moves upwards. It passes through the enthalpy tower channels and exchanges heat and mass with the liquid desiccant sprayed from above. Then, the air reaches point 3, and passing through the eliminator and trapping the solution particles along with the air, moves and reaches point 4. In addition, to prevent the carryover of the exhaust air, the enthalpy exchanger's channels were wicked, and the pumps were controlled to be on for 10 seconds and then off for 50 seconds. Now the air exits from the system through port 5 using the air pump. In the water flow path, first, the water is received

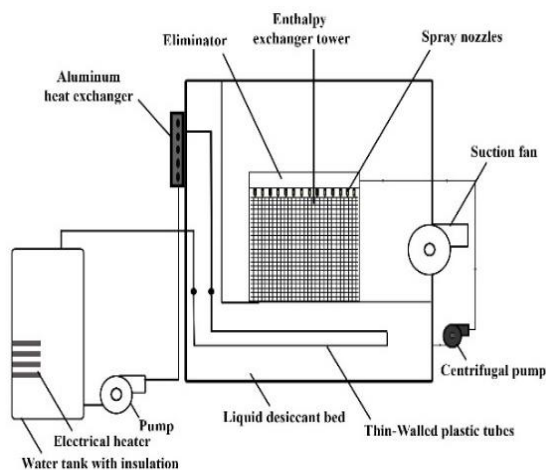


**Figure 3.** A schematic of the Liquid Desiccant Air Conditioner System consisting Absorbent Tower, Suction Fan, and Water tank

by the pump from point 6 or the water tank outlet and is transferred to the inlet of the aluminium heat exchanger or point 7. The water flow passes through the aluminium heat exchanger and transfers heat to the inlet air. Then, it leaves the aluminium heat exchanger through port 8 and reaches the liquid desiccant bed. After passing through the thin-walled plastic tubes in the bed of liquid desiccant, it also exchanges heat with the liquid desiccant and exits from port 9 and then returns to the water tank. In the water tank, water was heated by three electrical heaters in the regeneration process. But, in the dehumidification process, the heaters were turned off, and the water was cooled by adding 10 kg of ice at  $0^\circ \text{C}$ .

The liquid desiccant flow path is also shown in Figure 5. First, the liquid desiccant exits from the liquid desiccant bed by two centrifugal pumps made of polymeric materials and is transferred from point 10 to point 11. After passing through a suitable filter and the pipes and reaching the spray pipes at point 12, the solution is sprayed downwards. The liquid desiccant moves down through the channels by gravity and then, by contacting the processed air, which is moved from downwards to upwards, the heat and mass transfer occurs. Now, the solution reaches point 13 and returns to the liquid desiccant bed. It is worth mentioning that during the dehumidification process, cold water flowed in the direction of the aluminium heat exchanger and thin-walled plastic tubes for pre-cooling. Also, during the regeneration process, hot water flowed in the path of the aluminium heat exchanger and thin-walled plastic tubes for pre-heating. In the design of the experimental setup, there was one enthalpy exchanger. As a result, the dehumidification and regeneration processes were performed in two separate durations. The experiments were designed as follows:

1. Dehumidification process (pre-cooled air and liquid desiccant simultaneously).
2. Regeneration process (pre-heated air and liquid desiccant simultaneously).

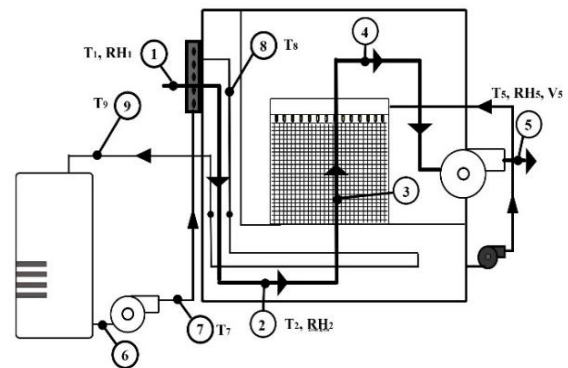


**Figure 4.** The direction of airflow, water flow and position of measuring instruments on the LDAC system

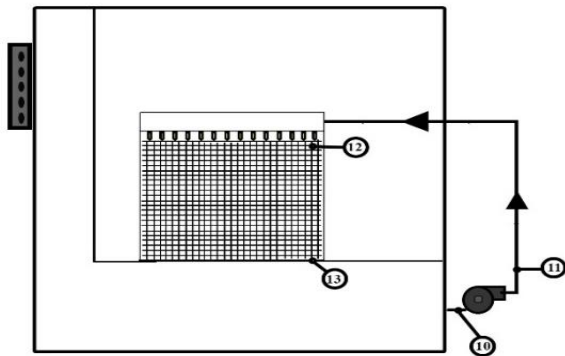


Figure 5. The direction of LiCl flow on the LDAC system

3. MEASUREMENT INSTRUMENTS

In this experiment, there were thermometer, thermocouples with data logger, air humidity meter, airflow velocity meter, and conductivity meter to measure the variation of temperature, relative humidity, airflow velocity and solution concentration, respectively. The position of measurement devices is shown in Figure 4. In addition, the solution concentration was measured before and after each process. The inaccuracy analysis of these measurement instruments is listed in Table 1, in which the expanded uncertainties have a confidence level of 95%.

4. EXPERIMENTAL RESULTS AND DISCUSSION

4. 1. Dehumidification Process In the dehumidification process, air and liquid desiccant were pre-cooled simultaneously. During the process,  $\dot{V}_5$  was 12.1 m/s. According to Figure 6, it is observed that  $T_7$  was about 11.8 °C during the process. Due to the heat transfer from the inlet air to the cooling water inside the

aluminium heat exchanger, the water temperature increases, and  $T_8$  reaches the average of 17.6 °C. Then, the water passed through the liquid desiccant bed, and the water temperature increased, and the mean of  $T_9$  reached about 17.9 °C. The dehumidification process was an exothermic reaction;  $T_5$  was higher than  $T_2$  and reached an average temperature of 27°C, which was approximately 14.64% on average higher than  $T_2$ .  $T_1$  was almost 30.2°C during the process, but  $T_2$  and  $T_5$  were decreased by about 29% and 21.1% during the dehumidification process.

The  $RH_1$  decreased slightly from 58.9% to 56.5% during the process. Then, as the air passes through the cold heat exchanger, the air relative humidity increased, which  $RH_2$  was an average of about 66.7%. Then, by passing air through the enthalpy exchanger and exchanging the moisture content with the solution, its relative humidity was reduced, which  $RH_5$  was an average of 56%.

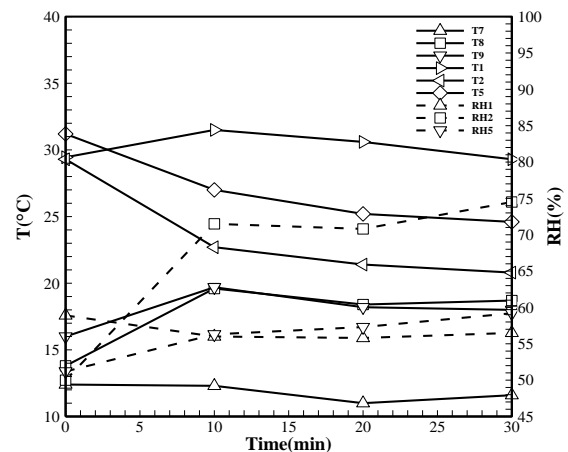


Figure 6. Temperature and relative humidity versus time in the dehumidification process

TABLE 1. The specification of measurement devices

Type	Accuracy	Expanded Uncertainty
1-Digital air thermometer model IDR-RH101.	± 0.1 °C	2.003°C
2-K type thermocouple with Lutron datalogger	± 0.1 °C	2.003°C
3-Digital air humidity meter model IDR-RH101.	± 0.1 %	2 %
4-Digital airflow velocity meter Omega HHF11A.	± 0.1 m/s	2.003 m/s
5-Conductivity meter for measuring the liquid desiccant concentration Orion Research Model 101.	± 0.1 ms/cm [msimense/cm].	1.006 ms/cm

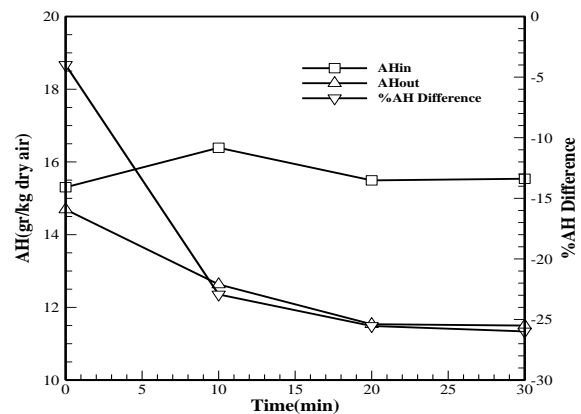


Figure 7. Absolute humidity versus time in the dehumidification process

Based on the psychrometric chart, the air absolute humidity (or moisture content) was obtained. Figure 7 displays the moisture content of the inlet air and the exhaust air and the percentage of their difference. AH<sub>5</sub> was less than AH<sub>1</sub>, and their difference was decreased from -3.9% to -25.9% during the dehumidification process. Therefore, the moisture content was reduced during the process, and the solution absorbed the moisture content of the inlet air. It is observed that the absolute humidity of the exhaust air has a higher rate at the beginning, and by the time and passing through the transition mode, it tends towards a certain amount equal to 11 g/kg of dry air. This is the same for the percentage difference between the absolute humidity of the inlet and exhaust air, and its value tends to be about -26% after about 30 minutes.

**4. 2. Regeneration Process** In the regeneration process, air and liquid desiccant were preheated simultaneously.  $\dot{V}_5$  was on about 10.73 m/s during the process. Figure 8 depicts that T<sub>7</sub> was from 41.7 °C to 50.9 °C during the process. Due to the heat transfer from the hot water inside the aluminium heat exchanger to the inlet air, the temperature decreased, and T<sub>8</sub> reached the average of 44.1 °C. Then, by heat transferring of water with liquid desiccant after passing through thin-walled plastic tubes, the water temperature decreased, and the mean of T<sub>9</sub> reached about 41.6 °C. After heat exchanging with the inlet air and then with the solution, the hot water temperature dropped by about 9.42%. The inlet air passed through the aluminium heat exchanger, and the air temperature risen by about 5 °C on average. Since the regeneration process was endothermic, the T<sub>5</sub> was 1.4 °C lower than T<sub>2</sub> on average. In addition, T<sub>1</sub> was almost about 32.4 °C, but T<sub>2</sub> and T<sub>5</sub> increased by approximately 16.27 and 12.97% during the regeneration process.

RH<sub>1</sub> was almost about 55.8% during the process. Then, as the air passes through the warm heat exchanger, relative humidity decreased, which RH<sub>2</sub> was an average of 43.3%. Then, after exchanging the moisture content in the enthalpy exchanger, air relative humidity was increased, which RH<sub>5</sub> was a mean of 49.6%.

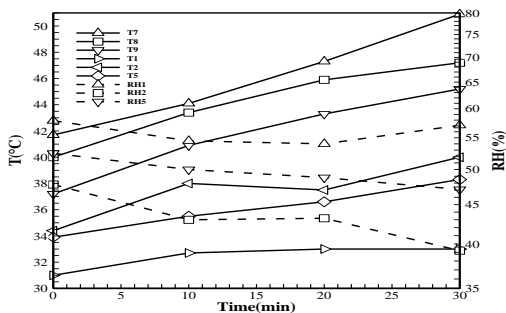


Figure 8. Temperature and relative humidity versus time in the regeneration process

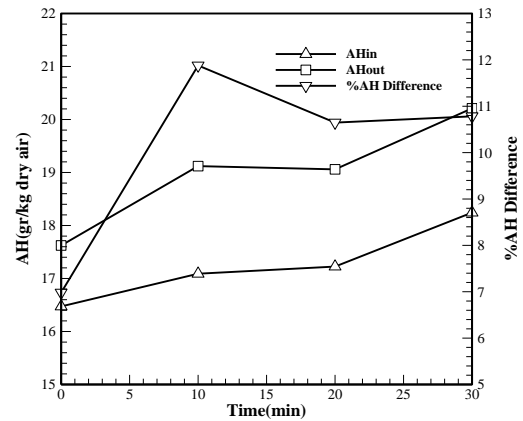


Figure 9. Absolute humidity versus time in the regeneration process

Figure 9 depicts the moisture content of the inlet air, and the exhaust air and the percentage of their difference. AH<sub>1</sub> was less than AH<sub>5</sub> and the percentage difference was increased from 6.9 to 10.7% during the regeneration process. Therefore, the moisture content was enhanced during the process, and the solution was regenerated. It is indicated that by the time and passing through the transition mode, the percentage difference between the absolute humidity of the inlet and exhaust air tends to be about 11%.

**4. 3. System Transient.Behavior** The PSO algorithm was used to fit a simulation curve to the dehumidification and regeneration rates and identify the transient behavior of the system [17, 18]. Research on various issues has been done utilizing this optimization algorithm [19, 20]. The fundamental of this algorithm is information sharing which is particle experiences. In the PSO algorithm, there are plenty of hypothetical particles that are distributed in the search domain, and they follow personal experiences and global experiences. There are two essential equations in the PSO algorithm as follows [21]:

$$x_{t+1}^i = x_t^i + v_{t+1}^i \tag{1}$$

$$v_{t+1}^i = w^i \times v_t^i + c_1 \times r_1 \times (p_t^i - x_t^i) + c_2 \times r_2 \times (p_t^g - x_t^i) \tag{2}$$

$x$ ,  $v$ ,  $w$ ,  $c_1$ ,  $c_2$ ,  $r_1$ ,  $r_2$ , and  $p^g$  are position, velocity, weight coefficient, the first coefficient, second coefficient, the first random number, the second random number and the best global position, respectively. In Equation (2), the next direction of the  $i$ th particle is determined according to the past direction, the best personal record and the best global record. In addition, the target was to reduce the difference between experimental data and fitted curve data in the cost function of this algorithm. An exponential

power series was used as an equation with fitting parameters as follows:

According to Equation (3), there are eight fitting parameters ( $a_1$ - $a_8$ ). The value of each fitting parameters is listed in Table 2. The air dehumidification rate and solution regeneration rate are shown in Figures 9. The rate of both processes was related to the time (t), and the results indicate that curve fitting had a good agreement with the experimental data and 10. For 1000 iterations and 300 populations, the average error of the fitted curve was 10.43 and 1.52% for regeneration rate and dehumidification rate, respectively.

According to Figure 10, the dehumidification rate curve had a downward trend. It tended to a particular value over time, which indicates that the device reached a steady state after approximately 10 minutes. The average dehumidification rate was equal to -14.76 kg/h. Also, Figure 11 shows that the regeneration rate curve had an upward trend, and it tended to a certain value over time, which indicates that the device reached near to steady-state after approximately 10 minutes. The average regeneration rate was equal to 7.18 kg/h.

$$\dot{m}_{water}(t) = a_1 \times \exp(a_2 \times t) + a_3 \times \exp(a_4 \times t) + a_5 \times \exp(a_6 \times t) + a_7 \times \exp(a_8 \times t) \tag{3}$$

TABLE 2. Variable coefficient of the fitted equation

Coeff	a1	a2	a3	a4	a5	a6	a7	a8
Deh. rate	22.821	19.163	41.628	0.282	-47.752	0.734	-19.578	0
Reg. rate	-12.281	0.381	-1.273	0.573	8.210	0.001	7.5452	0.578

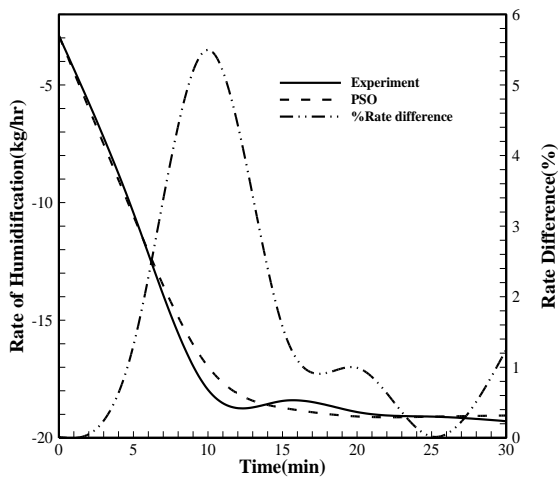


Figure 10. Curve fitting of the water flow rate of dehumidification with PSO

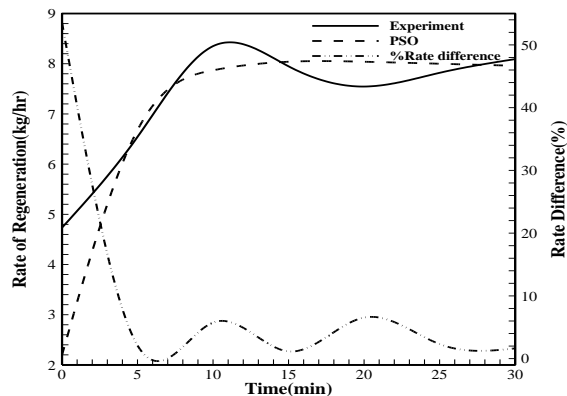


Figure 11. Curve fitting of the water flow rate of regeneration with PSO

### 5. COMPARISON WITH PREVIOUS STUDY

In the research conducted by Qiu et al.[10], relative humidity reduction during dehumidification process reached approximately 10% after 30 minutes. In this study, this amount is around 5% and one of the reason for it is high ambient relative humidity level in the experiment of Qiu et al.[10]. According to figures 7 and 9, the exhaust air moisture content reduced during the dehumidification process on average of 18.21%. But, about 9.78% on average was added to the exhaust air moisture content in the regeneration process. In the previous system[15], where the enthalpy exchanger and the eliminator were both wicked, the regeneration and dehumidification processes variation were on average of 34.07 and 8.29%, respectively. Also, in the case study where the enthalpy exchanger and the eliminator were both wicked, as well as the centrifugal pumps switcher was at the optimal frequency, the regeneration and dehumidification processes variation were on average of 20.54 and 7.25%, respectively.

### 6. CONCLUSION

In this study, a novel configuration of an LDAC with LiCl liquid desiccant was experimentally investigated. According to this configuration, inlet air and liquid desiccant was precooled during the dehumidification process and inlet air and liquid desiccant was preheated during the regeneration process, simultaneously. Additionally, PSO algorithm was utilized to estimate transient behavior of the system in the dehumidification and regeneration processes. The following results are concluded:

- In the exothermic reaction between processed-air and LiCl during the dehumidification process, exhaust air temperature was approximately 14.64% on average higher than processed-air temperature and it was decreased by about 21.1% during this process. In addition, the ambient air moisture content was reduced around 20% during the process, and the solution absorbed the moisture content of the inlet air.
- In the endothermic reaction between processed-air and LiCl during the regeneration process, exhaust air temperature was approximately 1.4 °C on average lower than processed-air temperature and it was increased by about 12.97% during this process. Furthermore, the ambient air moisture content was enhanced around 14.28% during the process, and the solution was regenerated.
- The exhaust air moisture content variation in dehumidification and regeneration processes was -18.21 and 9.78%, respectively.
- It was observed that the dehumidification and regeneration rates were equal to -14.76 kg/h and 7.18 kg/h on average, respectively.
- The PSO algorithm was used to fit a curve on the dehumidification and regeneration rate curves, which had a good agreement with experimental data and the average error of the fitted curve was 10.43 and 1.52% for regeneration rate and dehumidification rate, respectively.
- It is observed that this moisture content in the dehumidification process was improved by at least 9.92% than the previous study. However, the previous system performed at least about 10.76% better than this system in the regeneration process, which had three electrical heaters to warm the inlet air.

In future study, solar collectors and photovoltaic panels can improve the efficiency of the experimental setup and minimize the dependence on the grid power.

## 7. REFERENCES

1. Lowenstein, A.J.H. and Research, R., "Review of liquid desiccant technology for hvac applications", *HVAC&R Research* Vol. 14, No. 6, (2008), 819-839, doi: 10.1080/10789669.2008.10391042
2. Sahlot, M. and Riffat, S.B.J.I.J.o.L.-C.T., "Desiccant cooling systems: A review", *International Journal of Low-Carbon Technologies* Vol. 11, No. 4, (2016), 489-505, doi: 10.1093/ijlct/ctv032
3. Rafique, M.M., Gandhidasan, P., Bahaidarah, H.M.J.R. and Reviews, S.E., "Liquid desiccant materials and dehumidifiers—a review", *Renewable and Sustainable Energy Reviews*, Vol. 56, No., (2016), 179-195, doi: 10.1016/j.rser.2015.11.061
4. Baniyounes, A.M., Ghadi, Y.Y., Rasul, M., Khan, M.M.K.J.R. and Reviews, S.E., "An overview of solar assisted air conditioning in queensland's subtropical regions, australia", *Renewable and Sustainable Energy Reviews* Vol. 26, (2013), 781-804, doi: 10.1016/j.rser.2013.05.053
5. Verma, A., Kaushik, S., Tyagi, S.J.H. and Journal, I., "Thermodynamic analysis of a combined single effect vapour absorption system and tc-co2 compression refrigeration system", *HighTech Innovation Journal*, Vol. 2, No. 2, (2021), 87-98, doi: 10.28991/HIJ-2021-02-02-02
6. Assari, M.R., Mirzavand, R., Tabrizi, H.B. and Gholi Beik, A.J., "Effect of steps height and glass cover angle on heat transfer performance for solar distillation: Numerical study", *International Journal of Engineering, Transactions A: Basics*, Vol. 35, No. 1, (2022), doi: 10.5829/ije.2022.35.01a.23
7. Ha, K.J.H. and Journal, I., "Innovative blade trailing edge flap design concept using flexible torsion bar and worm drive", *HighTech Innovation Journal*, Vol. 1, No. 3, (2020), 101-106, doi: 10.28991/HIJ-2020-01-03-01
8. Alizadeh, S. and Saman, W.J.S.E., "Modeling and performance of a forced flow solar collector/regenerator using liquid desiccant", *Sol. Energy* Vol. 72, No. 2, (2002), 143-154, doi: 10.1016/S0038-092X(01)00087-1
9. Alizadeh, S. and Saman, W.Y.J.S.E., "An experimental study of a forced flow solar collector/regenerator using liquid desiccant", *Solar Energy* Vol. 73, No. 5, (2002), 345-362, doi: 10.1016/S0038-092X(02)00116-0
10. Qiu, G., Liu, H. and Riffat, S.B.J.I.J.o.L.-C.T., "Experimental investigation of a liquid desiccant cooling system driven by flue gas waste heat of a biomass boiler", *International Journal of Low-Carbon Technologies*, Vol. 8, No. 3, (2013), 165-172, doi: 10.1093/ijlct/cts003
11. Turgut, O.E., Çoban, M.T.J.H. and Transfer, M., "Experimental and numerical investigation on the performance of an internally cooled dehumidifier", *Heat Mass Transfer* Vol. 52, No. 12, (2016), 2707-2722, doi: 10.1007/s00231-016-1782-9
12. Mohamed, A., Ahmed, M., Hassan, A. and Hassan, M.S.J.C.S.i.T.E., "Performance evaluation of gauze packing for liquid desiccant dehumidification system", *Case Studies in Thermal Engineering* Vol. 8, (2016), 260-276, doi: 10.1016/j.csite.2016.08.005
13. Peng, D.-g., Li, S.-y., Luo, D.-t., Fu, Y.-t., Cheng, X.-s. and Liu, Y.J.J.o.Z.U.-S.A., "Efficiency comparison and performance analysis of internally-cooled liquid desiccant dehumidifiers using licl and CaCl<sub>2</sub> aqueous solutions", *Journal of Zhejiang University-Science A* Vol. 21, No. 1, (2020), 44-63, doi: 10.1631/jzus.A1900241
14. Lu, J., Wang, M., Li, Y. and Yang, L.J.P.E., "Numerical study on dehumidification performance of a cross-flow liquid desiccant air dehumidifier", *Procedia Engineering* Vol. 205, (2017), 3630-3637, doi: 10.1016/j.proeng.2017.10.221
15. Moazemi Goudarzi, A., Alizadeh, S., Ramezanzadeh, H.J.J.o.R.E. and Environment, "Experimental investigation of a new enthalpy exchanger with low absorbent carryover designed for liquid desiccant dehumidification system", *Journal of Renewable Energy and Environment* Vol. 4, No. 4, (2017), 22-30, doi: 10.30501/JREE.2017.88329
16. Hassan, F.A.J.J.o.H., Earth, and Future, "Multi-criteria approach and wind farm site selection analysis for improving power efficiency", *Journal of Human, Earth, Future* Vol. 1, No. 2, (2020), 60-70, doi: 10.28991/HEF-2020-01-02-02
17. Sadeghi, S.M.M., Hoseini, S., Fathi, A. and Daniali, H.M.J.I.J.o.E., "Experimental hysteresis identification and micro-position control of a shape-memory-alloy rod actuator", *International Journal of Engineering, Transactions A: Basics* Vol. 32, No. 1, (2019), 71-77, doi: 10.5829/ije.2019.32.01a.09
18. Bagheri, A., Sadafi, M. and Safikhani, H.J.I.J.o.E., "Multi-objective optimization of solar thermal energy storage using hybrid of particle swarm optimization and multiple crossover and

- mutation operator", *International Journal of Engineering, Transactions B Applications* Vol. 24, No. 4, (2011), 367-376, doi: 10.5829/idosi.ije.2011.24.04b.07
19. Aslipour, Z. and Yazdizadeh, A.J.I.J.o.E., "Identification of wind turbine using fractional order dynamic neural network and optimization algorithm", *International Journal of Engineering, Transactions B Applications* Vol. 33, No. 2, (2020), 277-284, doi: 10.5829/ije.2020.33.02b.12
20. Nahvi, H. and Mohagheghian, I.A., "Particle swarm optimization algorithm for mixed variable nonlinear problems", *International Journal of Engineering, Transactions A, Basics*, Vol. 24, (2011), 65-78, doi:
21. Jam, S., Shahbahrani, A. and Sojoudi Ziyabari, S.J.I.J.o.E., "Parallel implementation of particle swarm optimization variants using graphics processing unit platform", *International Journal of Engineering, Transactions A, Basics* Vol. 30, No. 1, (2017), 48-56, doi: 10.5829/idosi.ije.2017.30.01a.07

---

### Persian Abstract

---

#### چکیده

مایعات خورنده مانند لیتیوم کلرید در تهویه مطبوع با خشک کن مایع استفاده می شود. خوردگی در مبدل آنتالپی یکی از مشکلات طراحی است. برخی از راه حل ها در این تحقیق مورد مطالعه قرار گرفته و بر اساس آنها، یک سیستم آزمایشگاهی بطور تجربی بررسی شده است. در این طرح، از مبدل آنتالپی جریان مخالف برای تبادل رطوبت بین هوا و خشک کن مایع استفاده می شود. ابتدا هوای ورودی توسط مبدل حرارتی آلومینیومی از قبل گرم یا از قبل سرد می شود. سپس، خشک کن مایع توسط لوله های پلاستیکی دیواره نازک از قبل گرم یا سرد می شود. با تماس این مایع خشک کن و هوا، تبادل گرما و جرم اتفاق می افتد. تغییرات محتوای رطوبت هوا در شرایط آزمایشگاهی بررسی شده و میزان احیا و رطوبت زدایی مورد مطالعه قرار می گیرد. نتایج حاکی از آن است که به طور کلی میزان رطوبت هوای محیط در طی فرآیند رطوبت زدایی، حدود ۲۰ درصد کاهش و در طول فرآیند احیا، حدود ۱۴/۲۸ درصد افزایش یافت. علاوه بر این، تغییرات محتوای رطوبت در فرآیند رطوبت زدایی حداقل ۹/۹۲ درصد بهبود یافت، اما فرآیند احیا حداقل ۱۰/۷۶ درصد نسبت به مطالعه قبلی کاهش یافت. همچنین، استفاده از الگوریتم بهینه سازی ازدحام ذرات برای شناسایی رفتار گذرا سیستم و به دست آوردن پارامترهای برازش منحنی، شباهت زیادی با داده های تجربی میزان رطوبت زدایی و احیا دارد و میانگین خطای برازش منحنی به ترتیب ۱۰/۴۳ درصد و ۱/۵۲ درصد برای دو فرآیند شده است.

---